

Impurity effect as a probe for $s_{x^2-y^2}$ symmetry in iron based superconductors

Tao Zhou¹, Degang Zhang¹, Xiang Hu^{1,2}, Jian-Xin Zhu², and C. S. Ting¹

¹*Texas Center for Superconductivity and Department of Physics, University of Houston, Houston, Texas 77204*

²*Theoretical Division, Los Alamos National Laboratory, Los Alamos, New Mexico 87545, USA*

(Dated: December 22, 2018)

The local impurity states is calculated for a superconductor with $s_{x^2-y^2}$ pairing symmetry based on the minimal two band model proposed by S. Raghu *et al.* [Phys. Rev. B **77**, R220503 (2008)], and the self-consistent Bogoliubov-de Gennes equations. Since the quasiparticles can be scattered from the region with positive order parameter to the region with negative order parameter at different Fermi surface pockets, Andreev bound states should form inside the gap. As a result, two in-gap resonance peaks are found at or near the nonmagnetic impurity site. The presence of these in-gap states should be an indication for the existence of the sign reversal of the pairing order parameter. The effect due to a magnetic impurity is also presented.

Introduction The new family of superconducting materials which contain Fe-As layers has attracted much attention since their discovery [1]. The Fe-As layers are believed to be the conducting planes. The band calculations have shown that the Fermi surface includes two hole pockets centered at (0, 0) and two electron pockets centered at (π, π) , respectively [2, 3, 4], which is confirmed by angle-resolved photoemission spectroscopy (ARPES) experiments [5, 6, 7, 8, 9, 10]. A number of experiments have indicated that this family of materials is not conventional [11]. Thus probing the pairing symmetry is one of the most important issues since it can provide us the information of the pairing mechanism. However, this issue is still controversial and needs to be investigated further.

One popular proposal for the pairing symmetry is the s_{\pm} -wave gap [12, 13, 14, 15, 16], namely, the superconducting gap is extended s-wave and has opposite sign for the hole and electron pockets. Experimentally, the s-wave gap symmetry is supported by penetration depth measurement [17], ARPES [6, 7, 8, 9, 10] and specific heat measurement [18]. In particular, the gap magnitudes at different Fermi surface pockets measured by ARPES experiments agree well with $s_{x^2-y^2} = \cos k_x \cos k_y$ form (here k_x and k_y represent the momentum in the unfolded Brillouin zone) [8]. However, although ARPES experiments have been a powerful tool to measure the gap magnitude directly, it cannot determine the phase of the superconducting order parameter. Detecting the phase of order parameter is an essential and important step to map out the gap symmetry. Recently several theoretical works propose different ways to measure the sign change of the gap [19, 20, 21, 22, 23]. However, for multiband materials, probing the phase of the order parameter is a quite challenge task. So far there is no direct and powerful methods.

The impurity effect has been an important part in the studies of the superconductivity [24]. The effect of impurity scattering is sensitive on the symmetry of order parameter, thus it is a useful tool to probe the pairing symmetry. A well-known result of d -wave pairing in the cuprates is the zero bias peak in the local density of states (LDOS) near the nonmagnetic impurity site. The zero bias peak is suggested to be caused by the Andreev reflection due to the opposite phase of the order parameter [25]. Such zero energy bound state will not exist in isotropic s-wave superconductors. For the case of iron-based materials, if the pairing symmetry is s_{\pm} type, similar Andreev bound states are expected to exist due to the interband scat-

tering. In fact, based on the analytic T -matrix approach and a four band model, three of the present authors calculated the LDOS near the impurity site and do find the sharp resonance peaks inside the gap [26]. The peaks will disappear if the phase of the order parameter is taken to be the same. Furthermore, the characteristic of the resonance peaks is significantly different with the cases of d -wave or nodal s -wave, namely, since we consider the nodeless case, there is no quasiparticle scattering at very low energies. Thus the in-gap bound states are actually located at the positive and negative energies and the LDOS tends to be zero at low energies. The impurity effect is expected to be sensitive to the detailed band structure [24]. The sensitivity maybe more remarkable for the multi-band materials. Since the calculation in Ref. [26] is based on a band structure which artificially fits the ARPES experiments [27, 28], in the present paper we wish to examine the LDOS at and near the impurity site based on a different two-band model as proposed by Raghu *et al.* [29], and the self-consistent Bogoliubov-de Gennes (BdG) equations. Under the present approach, the gap magnitude is expected to be suppressed at and near the impurity site. It is proposed that such suppression effect needs to be taken into account to study the local impurity states [30]. Our numerical results show that the feature of in-gap states is robust despite what kind of band structure we used, but the detailed spectra of the local impurity states are quite different and sensitive to the parameters for obtaining the band structure. For a nonmagnetic impurity with positive scattering potential, we obtain two in-gap resonance peaks. The resonance peaks locate near the coherent peaks for weak potentials and move to lower energy as the potential increases. The weight of the resonance peak with positive energy becomes very pronounced as the scattering potential reaching the unitary limit. For the cases of negative scattering potentials, the in-gap resonance peaks are moving away from the coherent peaks and are closer to the zero energy. The position of the resonance peaks are robust and depend weakly on the scattering potentials. All other features remain practically the same. We also study the impurity states for a magnetic impurity, the feature is similar to that in a typical s -wave superconductor [31, 32, 33]. Experimentally the LDOS can be measured by scanning tunneling microscopy (STM) experiments., and thus is a direct tool to probe the pairing symmetry of this family of compounds.

Model and formalism As we mentioned above, iron-based

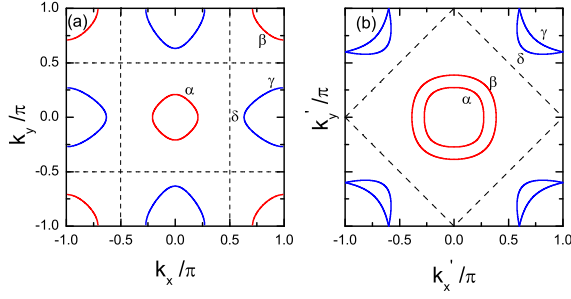


FIG. 1: (Color online) The Fermi surface in the extended Brillouin zone and folded Brillouin zone respectively. The dashed lines are nodal lines for $s_{x^2y^2}$ wave. The (thin) red and (bold) blue colors represent the hole and electron pockets, respectively.

superconducting materials have a layered structure. In the FeAs layer there are two Fe ions per unit cell by taking into account As ions located above or below the Fe-Fe plane. The band calculations have shown that the main features of the bands that determine the Fermi surface are the two orbitals d_{xz} and d_{yz} [34, 35]. We here use a two band model considering the two degenerate orbitals per cite [29]. The model Hamiltonian reads,

$$H = H_t + H_\Delta + H_{imp}, \quad (1)$$

where H_t is the hopping term,

$$H_t = - \sum_{i\mu j\nu\sigma} (t_{i\mu j\nu} c_{i\mu\sigma}^\dagger c_{j\nu\sigma} + h.c.) - t_0. \quad (2)$$

where i, j are the site indices and $\mu, \nu = 1, 2$ are the orbital indices. t_0 is the chemical potential.

H_Δ is the pairing term,

$$H_\Delta = \sum_{i\mu j\nu\sigma} (\Delta_{i\mu j\nu} c_{i\mu\sigma}^\dagger c_{j\nu\sigma}^\dagger + h.c.). \quad (3)$$

H_{imp} is the impurity term expressed by,

$$H_{imp} = v_s \sum_{i\mu\nu\sigma} c_{i\mu\nu\sigma}^\dagger c_{i_m\nu\sigma} + v_m \sum_{i_m\nu} (c_{i_m\nu\uparrow}^\dagger c_{i_m\nu\uparrow} - c_{i_m\nu\downarrow}^\dagger c_{i_m\nu\downarrow}), \quad (4)$$

v_s term represents the nonmagnetic impurity and v_m term is the magnetic impurity.

The Hamiltonian can be diagonalized by solving the BdG equations self-consistently,

$$\sum_j \sum_\nu \begin{pmatrix} H_{i\mu j\nu} & \Delta_{i\mu j\nu} \\ \Delta_{i\mu j\nu}^* & -H_{i\mu j\nu}^* \end{pmatrix} \begin{pmatrix} u_{j\nu\sigma}^n \\ v_{j\nu\bar{\sigma}}^n \end{pmatrix} = E_n \begin{pmatrix} u_{i\mu\sigma}^n \\ v_{i\mu\bar{\sigma}}^n \end{pmatrix}, \quad (5)$$

where the Hamiltonian $H_{i\mu j\nu}$ is expressed by,

$$H_{i\mu j\nu} = -t_{i\mu j\nu} + (v_s \delta_{i,i_m} - t_0 + \sigma v_m \delta_{i,i_m}) \delta_{ij} \delta_{\mu\nu}. \quad (6)$$

The superconducting order parameter and the local electron density $n_{i\mu}$ satisfy the following self-consistent conditions,

$$\Delta_{i\mu j\nu} = \frac{V_{i\mu j\nu}}{4} \sum_n (u_{i\mu\uparrow}^n v_{j\nu\downarrow}^{n*} + u_{j\nu\uparrow}^n v_{i\mu\downarrow}^{n*}) \tanh\left(\frac{E_n}{2K_B T}\right), \quad (7)$$

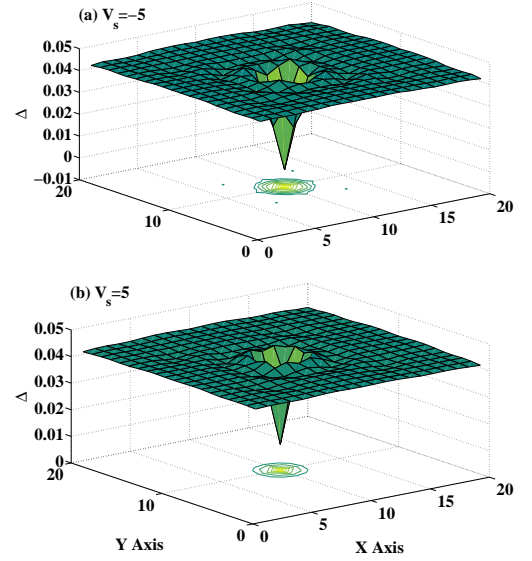


FIG. 2: (Color online) Amplitudes of the order parameter in presence of a single nonmagnetic impurity.

$$n_{i\mu} = \sum_n |u_{i\mu\uparrow}^n|^2 f(E_n) + \sum_n |v_{i\mu\downarrow}^n|^2 [1 - f(E_n)]. \quad (8)$$

Here $V_{i\mu j\nu}$ is the pairing strength and $f(x)$ is the Fermi distribution function.

The LDOS is expressed by,

$$\rho_{i\sigma}(\omega) = \sum_{n\mu} [|u_{i\mu\sigma}^n|^2 \delta(E_n - \omega) + |v_{i\mu\bar{\sigma}}^n|^2 \delta(E_n + \omega)], \quad (9)$$

where the delta function $\delta(x)$ is taken as $\Gamma/\pi(x^2 + \Gamma^2)$. The supercell technical is used to calculated the LDOS.

In our following calculation, we use the hoping constant suggested by Ref. [29], where t_{1-3} are the hoping between the same orbitals and t_4 represents the hoping between different orbitals. t_4 has opposite sign along different direction. $t_{1-4} = -1, 1.3, -0.85, -0.85$. t_0 is determined by the doping density. The Fermi surface with filling electron density 2.1 per site is plotted in Fig.1(a). Alternatively, if we consider one unit cell contains two Fe ions, the Fermi surface in the reduced Brillouin zone is plotted in Fig.1(b).

Our work will focus on the characteristic of s_\pm symmetry. In order to reproduce the s_\pm -wave, we consider the pairing between the same orbital of the next nearest neighbor site. Without the impurity, self-consistent calculation verified that this kind of pairing produces s -wave gap symmetry, i.e., $\Delta_{i\mu, i\pm\hat{x}\pm\hat{y}\mu} \equiv \Delta_0$. Transforming the Hamiltonian to the momentum space and diagnizing the 4×4 Hamiltonian, it is easy to verify that the pairing symmetry is exactly the same with the $s_{x^2y^2}$ -symmetry proposed by Ref. [36], namely, the gap function in the extended Brillouin zone has $\cos k_x \cos k_y$ form, and has the form of $\cos k'_x + \cos k'_y$ in the reduced Brillouin zone. The nodal line of the gap function is shown in Fig.1.

In the following presented results, we choose the filling electron density $n = 2.1$ per site (electron doped samples with doping $\delta = 0.1$) and pairing potential $V = 1.2$. These param-

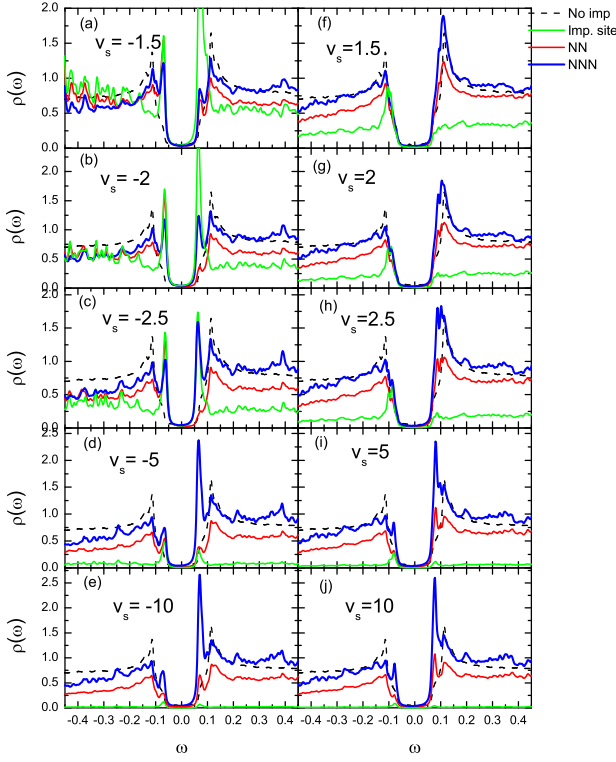


FIG. 3: (Color online) The LDOS spectra in presence of a single nonmagnetic impurity for different scattering potentials with quasi-particle damping $\Gamma = 0.004$. The (green) dash-dotted lines are the LDOS at the impurity site. The thin (red) solid and bold (blue) solid lines are the spectra at nearest neighbor and next nearest neighbor sites to the impurity. The dotted lines are the density of states without the impurity.

ters are chosen just for illustration. We have checked numerically that our main results are not sensitive to the parameters.

Nonmagnetic impurity scattering We first illustrate the feature of single nonmagnetic impurity scattering, namely, $v_s \neq 0$ and $v_m = 0$. In real materials, both negative and positive scattering potentials are possible. Thus here we discuss both cases. The numerical calculation is performed on 20×20 lattice. The impurity is put at the site (10, 10). And a 80×80 supercell is taken to calculate the LDOS.

We plot the self-consistently determined gap amplitudes on the lattice ($\Delta_i = \frac{1}{8} \sum_{j\mu} \Delta_{i,j\mu}$) in Fig.2 for $v_s = \pm 5$. As seen, the gap is suppressed near the impurity and quite small at the impurity site. It will recover to the uniform value at about $2 \sim 3$ lattice spacings from the impurity site. Note that the gap suppression effect is more notable for the negative potential.

The LDOS spectra for different scattering potentials at and near the impurity sites are plotted in Fig.3. As seen, the left panels are the negative potential cases. Obvious impurity states exist at the energy about $\pm 0.57\Delta$ (here Δ is the energy of the superconducting coherent peak). The energy of the impurity resonance peaks depends weakly on the scattering potential v_s . At the impurity site, for weak scattering potential v_s , two sharp resonances peaks inside the gap are shown, and the resonance peaks are suppressed as v_s increases and the LDOS

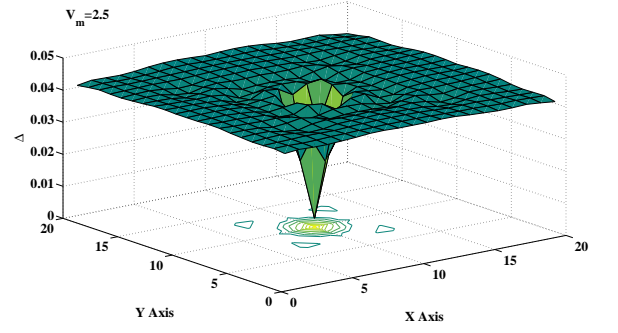


FIG. 4: (Color online) Amplitudes of the order parameter in presence of a single magnetic impurity.

tends to zero at the unitary limit. On the other hand, near the impurity site, the in gap resonance peaks show up and the intensity increases as the potential v_s increases. The resonance peaks are remarkable at the next nearest neighbor site. And in the unitary limit, a very sharp and strong resonance peak appear at the positive energy for the LDOS at the next nearest neighbor site of the impurity site. This situation may qualitatively correspond to the case for a charged Ba^{+2} impurity with a negative or attractive potential seen by electrons on the FeAs layer. This type impurity may present in the FeAs layer when $\text{BaFe}_{2-x}\text{Co}_x\text{As}_2$ is used for STM experiments [37].

The right panels show the effect of positive scattering potential impurity. As seen, we do not see clear resonance peaks at the impurity site even for the weak potential, which is different as that of the negative potential. Near the impurity site, similar as the case of the negative potential, the in gap resonance peaks show up as the potential increases, while the intensities seem to be smaller than those of the negative potential impurities. And the resonance peaks are more remarkable at the next nearest neighbor site, which is similar as that of the negative potential. It is also needed to point out that the positions of the two resonance peaks are much closer to the coherent peaks for weak scattering potentials. The intensity of the resonance peaks with positive energy increase and the positions move away from the superconducting coherent peaks to lower energies as the scattering potential increases. For a quite strong impurity scattering potential ($v_s = 10$), the in gap peaks locate at the energy about $\pm 0.7\Delta$. The spectrum is quite similar as that of the negative potential ($v_s = -10$).

On the whole, the in gap states here we obtained are quite robust for a strong impurity. The origin of them is mentioned above and discussed in Ref. [26]. It is due to the scattering between the different Fermi surface pockets. Because the order parameter has opposite sign between the hole-like pockets and electron-like pockets. Thus the inter band scattering can be seen as a superconductor-normal-superconductor junction with a relative phase shift, which leads to the Andreev bound states. As a result, we propose that this can be used to detect the sign reversal of the order parameter.

Magnetic impurity We now turn to study the effect of single magnetic impurity. We consider the exchange coupling to the impurity spin $v_m \neq 0$ and neglect the potential scattering strength v_s . The impurity is put at the site (10, 10). And a

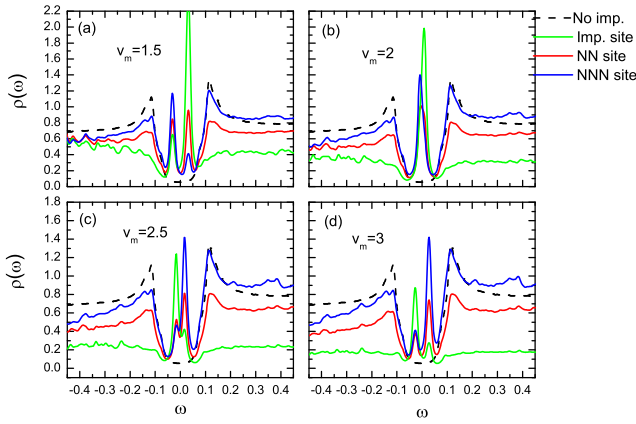


FIG. 5: (Color online) The LDOS spectra in presence of a single magnetic impurity site for different scattering potentials with quasi-particle damping $\Gamma = 0.008$. The dash-dotted (green) lines are the LDOS at the impurity site. The thin (red) and bold (blue) lines are the spectra at nearest neighbor and next nearest neighbor sites to the impurity. The dotted lines are the density of states without the impurity.

40×40 supercell is taken to calculate the LDOS.

The self-consistently determined gap amplitudes on the lattice is plotted in Fig.4 for $v_m = 2.5$. Similar as that of the nonmagnetic impurity case, the gap amplitudes are suppressed near the impurity site and recovered to the normal value at

about 3 lattice spacings to the impurity site.

The LDOS spectra with different magnetic potentials are plotted in Fig.5. As seen, at the impurity site, two resonance peaks exist and the superconducting coherent peak is invisible. The energy of the resonance peaks depend on the impurity potential and the two peaks merge into one peak at zero energy as the potential increases to $v_m = 2.0$. When v_m increases further the resonance peaks are separated again. Near the impurity site, the superconducting coherent peak can be seen clearly. The impurity states can also be seen clearly inside the gap. Note that such in gap states cannot be used to detect the sign reverse of the order parameter. The in gap states near the magnetic impurity are robust. They exist regardless of the pairing symmetry. In fact, the in gap states caused by the magnetic impurity are predicted in 1960s in conventional s -wave superconductors [31, 32, 33].

Summary We study the LDOS at and near the impurity site based on the self-consistent BdG equations, and The minimal two band model [29]. The in gap states are revealed near the impurity site. We propose that the in gap states near the non-magnetic impurity can be used as probe for the sign Reversal of the order parameter.

Acknowledgements The authors would like to thank S. H. Pan and Ang Li for useful discussions. This work was supported by the Texas Center for Superconductivity at the University of Houston and by the Robert A. Welch Foundation under the Grant no. E-1411.

-
- [1] Y. Kamihara *et al.*, J. Am. Chem. Soc. **130**, 3296 (2008).
 - [2] D. J. Singh and M. H. Du, Phys. Rev. Lett. **100**, 237003 (2008).
 - [3] S. Ishibashi, K. Terakura, and H. Hosono, J. Phys. Soc. Jpn. **77**, 053709 (2008).
 - [4] K. Nakamura, R. Arita, and M. Imada, J. Phys. Soc. Jpn. **77**, 093711 (2008).
 - [5] D. H. Lu *et al.*, Nature (London) **455**, 81 (2008).
 - [6] H. Ding *et al.*, Europhys. Lett. **83**, 47001 (2008).
 - [7] T. Kondo *et al.*, Phys. Rev. Lett. **101**, 147003 (2008).
 - [8] K. Nakayama *et al.*, Europhys. Lett. **85**, 67002 (2009).
 - [9] D. V. Evtushinsky *et al.*, Phys. Rev. B **79**, 054517 (2009).
 - [10] C. Liu *et al.*, Phys. Rev. Lett. **101**, 177005 (2008).
 - [11] For a review, see, e.g., Mikhail V Sadovskii, Phys. Usp. **51**, No. 12, 1201 (2008).
 - [12] I. I. Mazin, D. J. Singh, M. D. Johannes, and M. H. Du, Phys. Rev. Lett. **101**, 057003 (2008).
 - [13] A. V. Chubukov, D. V. Efremov, and I. Eremin, Phys. Rev. B **78**, 134512 (2008).
 - [14] Zi-Jian Yao, Jian-Xin Li, and Z. D. Wang, New J. Phys. **11**, 025009 (2009).
 - [15] Shun-Li Yu, Jing Kang, and Jian-Xin Li, Phys. Rev. B **79**, 064517 (2009).
 - [16] F. Wang, H. Zhai, Y. Ran, A. Vishwanath, and D.-H. Lee, Phys. Rev. Lett. **102**, 047005 (2009).
 - [17] K. Hashimoto *et al.*, Phys. Rev. Lett. **102**, 017002 (2009).
 - [18] Gang Mu, Huiqian Luo, Zhaosheng Wang, Lei Shan, Cong Ren, Hai-Hu Wen, arxiv: 0808.2941.
 - [19] Wei-Feng Tsai, Dao-Xin Yao, B. Andrei Bernevig, JiangPing Hu, arXiv:0812.0661.
 - [20] Pouyan Ghaemi, Fa Wang, Ashvin Vishwanath, Phys. Rev. Lett. **102**, 157002 (2009).
 - [21] David Parker and Igor Mazin, arxiv: 0812.4416.
 - [22] Jiansheng Wu and Philip Phillips, Phys. Rev. B **79**, 092502 (2009).
 - [23] Yan-Yang Zhang, Chen Fang, Xiaoting Zhou, Kangjun Seo, Wei-Feng Tsai, B. Andrei Bernevig, and Jiangping Hu, arxiv: 0903.1694.
 - [24] A. V. Balatsky, I. Vekhter, and Jian-Xin Zhu, Rev. Mod. Phys. **78**, 000373 (2006).
 - [25] Chia-Ren Hu, Phys. Rev. Lett. **72**, 1526 (1994).
 - [26] Degang Zhang, Tao Zhou, and C. S. Ting, arxiv: 0904.3708.
 - [27] Y. Sekiba *et al.*, New J. Phys. **11**, 025020 (2009).
 - [28] K. Terashima *et al.*, arxiv: 0812.3704.
 - [29] S. Raghu, Xiao-Liang Qi, Chao-Xing Liu, D. J. Scalapino, and Shou-Cheng Zhang, Phys. Rev. B **77**, 220503(R) (2008).
 - [30] Alexander Shnirman, Inanc Adagideli, Paul M. Goldbart, and Ali Yazdani, Phys. Rev. B **60**, 7517 (1999).
 - [31] L. Yu, Acta Phys. Sin. **21**, 75 (1965).
 - [32] H. Shiba, Prog. Theor. Phys. **40**, 435 (1968).
 - [33] A. I. Rusinov, JETP Lett. **9**, 85 (1969).
 - [34] L. Boeri, O. V. Dolgov, and A. A. Golubov, Phys. Rev. Lett. **101**, 026403 (2008).
 - [35] V. Vildosola, L. Pourovskii, R. Arita, S. Biermann, and A. Georges, Phys. Rev. B **78**, 064518 (2008).
 - [36] Kangjun Seo, B. A. Bernevig, and Jiangping Hu, Phys. Rev. Lett. **101**, 206404 (2008).
 - [37] S. H. Pan *et al.*, private communication.